The Statistical Characteristics of Convective Cells in a Monsoon Regime (Darwin, Northern Australia)

PETER T. MAY

Bureau of Meteorology Research Centre, Melbourne, Australia

ANDREW BALLINGER

Centre for Dynamic Meteorology, Monash University, Clayton, Australia

(Manuscript received 29 July 2005, in final form 10 April 2006)

ABSTRACT

A season of operational cell and track data from Darwin, Australia, has been analyzed to explore the statistical characteristics of the convective cell heights. The statistics for the monsoon and break regimes are significantly different with the break season cells being higher for a given reflectivity threshold. The monsoon cells produce more rain, but there are fewer intense cells and there is a much larger contribution from stratiform rain. The monsoon cells are also slightly larger, but shorter lived than the breaks. The shorter lifetime may reflect a more rapid transition to a longer-lived stratiform character. The monsoon regime is shown to be associated with large-scale ascent and higher humidity that may lead to more frequent, but weaker cells. Within regimes, the subset of intense cells generally reach near the tropopause or overshoot. However, there is little evidence in the data for a multimodal distribution of cell heights, except perhaps for the intense monsoon cases. Instead, the picture is a continuous distribution of cell heights with the peak of the distribution shifting to higher values as the distributions are conditioned on higher reflectivity.

1. Introduction

The height distribution of towering cumulus clouds has important implications for many characteristics of the tropical atmosphere. For example, the height and intensity of storms affect the upper-tropospheric temperature and humidity structure (e.g., Folkins 2002). The storm characteristics have important implications for tropospheric–stratospheric exchange and height distribution of the cirrus anvils that in turn have profound influences on the earth's radiation budget. There have been suggestions by Johnson et al. (1999) and May and Rajopadhyaya (1999) that there were two distinct modes of deep convection, one nearing the tropopause and the other "topping" in the region of 5–10 km (as well as a trade cumulus mode identified by Johnson et al. that is not relevant to the area being discussed). However, the May and Rajopadhyaya work did have a caveat that the "midlevel" mode was part of the life cycle of potentially deeper convection. This analysis was partly driven by the need to test these conjectures. The studies of Johnson et al., May and Rajopadhyaya, and Short and Nakamura (2000) as well as recent work by Goeke et al. (2005) all indicate the potential importance of relatively shallow convective systems, but the question of how these fit into the population of thunderstorm cells requires further study.

The maximum height that towering convection reaches in the Tropics has been studied using operational radar data from northern Australia. Operational radar storm cell tracks have been utilized and the maximum height that these cells reach in each "volume" scan has been recorded. This dataset has the advantage of being generated with an objective cell definition and automatic tracking allowing the sampling of large datasets. The tracking in particular allows us to select the maximum height and size that cells reach during their lifetime. While this is not perfect, it provides a large sample of data to further investigate issues arising

Corresponding author address: Dr. Peter T. May, Bureau of Meteorology Research Centre, GPO Box 1289, Melbourne VIC 3001, Australia.
E-mail: p.may@bom.gov.au

DOI: 10.1175/MWR3273.1

from the Johnson et al. and May and Rajopadhyaya work. The data have been separated into the "buildup and break" season when the convection is continental in character and therefore tends to be more intense and "monsoon" periods when the convection is oceanic in nature (e.g., Holland 1986; Drosdowsky 1996). It may be expected that the cells in these two regimes may have different characteristics. It has been observed that the break cells are very electrically active and have high reflectivities extending well above the freezing level (e.g., Williams et al. 1992; Rutledge et al. 1992; Keenan and Carbone 1992). Recent observations with polarimetric radar also show significant hail production in break cells (May and Keenan 2005). In contrast, the monsoon convection is more maritime in character with less electrical activity, rapid decrease of reflectivity above the freezing level, and little hail. This is all consistent with the break cells being more intense, at least in terms of the maximum vertical velocities being significantly greater in the midlevels. It is uncertain how this translates into the cell heights, although analysis of the Tropical Rainfall Measuring Mission (TRMM) data shows consistently higher storms with larger ice contents for continental convection compared to oceanic storms (Toracinta et al. 2002). It is important to note that the Johnson et al. paper was discussing observations over the open ocean during the Global Atmospheric Research Program (GARP) Atlantic Tropical Experiment (GATE) and Tropical Ocean Global Atmosphere Coupled Ocean–Atmosphere Response Experiment (TOGA COARE) and will therefore be expected to more closely correspond to the monsoon observations, but some differences are inevitable (e.g., Petersen and Rutledge 2001).

It will be shown that these two regimes have distinctly different height distributions with the break cells being consistently deeper and a higher percentage of intense cells. The distributions of cell height are continuous and single peaked with the exception of the monsoon intense cells showing some bimodality.

2. Datasets and methods of analysis

The impact of convection on the structure of the upper troposphere and on the cloud field depends on the depth of the convective clouds in the sampled synoptic regimes. This question will be examined using the Darwin, Australia, operational weather radar. This radar collects a three-dimensional volume of data out to a range of 150 km every 10 min. Each volume consists of a series of 16 conical sweeps at elevations ranging from 0.5° to 42°. The Australian Bureau of Meteorology uses an automatic objective cell identification and tracking system [the Thunderstorm Identification, Tracking, Analysis, and Nowcasting (TITAN); Dixon and Wiener 1993] on its radar systems. TITAN defines a cell as a contiguous volume of pixels that exceed a prescribed reflectivity threshold (35 and 45 dBZ are used here). A minimum cell volume of 30 km^3 is used to eliminate noisy data. The volume threshold will eliminate some true small cells, but manual inspection of images suggests that there are few cells that reach the reflectivity threshold and not the size threshold in the data used in this study. TITAN then tracks cells through successive volume scans using a combinatorial optimization procedure that is described in detail in Dixon and Wiener (1993). Where a cell splits or two cells merge, TITAN retains a simple track where the separate elements are tracked and a complex track where the cell is considered a single entity. That is where a split or merger occurs, the cell elements have the same cell identification. For this analysis we use these "complex" tracks to avoid ambiguity with regard to cell lifetimes and sizes, so for example, our cell maximum height is the greatest height attained at any stage of the cell evolution regardless if it is before or after a split or merger.

This system has been used to track and document the life cycle of storm cells through the November 2003–February 2004 wet season. Two sets of TITAN tracks were collected using reflectivity thresholds of 35 and 45 dBZ. The 35-dBZ storm cells capture most of the convective rain cells while the 45-dBZ threshold cells are the subset of intense cells. Several hundred of these cells have been tracked and the statistics were calculated over a period of 4 months. TITAN also keeps track of cell splits and mergers. For this analysis any cells that split or merged during their life cycle were treated as one cell. The database was extended by recording the profile of the maximum reflectivity in the area above the cell footprint as a function of height. This was done by constructing a series of the constant altitude plan position indicators (CAPPIs) every 1 km in height using a kriging procedure (Seed and Pegram 2001). While this may smear out the signals, a manual inspection of the resulting CAPPIs showed that the upper parts of deep intense cells looked reasonable, and there was no sign of artifacts produced by the radar scanning geometry with their nonoverlapping elevation angles and CAPPI construction such as rings of reflectivity. The CAPPIs were constructed on a 256 km $\times$ 256 km grid, so that some of the TITAN domain is excluded. Any tracks that passed outside the CAPPI domain were excluded from the storm-top height statistics, although they appear in the number of cells as a function of time.

Thus, for each cell we have a vertical profile of re-

flectivity for each 10-min radar volume. These data are then examined for rectangular regions above and enclosing the TITAN "cells" and the maximum height for reflectivities of 1, 5, 10, and 20 dBZ above the cells were recorded. Rectangles were used for ease of computation and to allow for some tilting and spreading of the cloud with height. These thresholds were chosen to provide a number of reasonable steps in reflectivity thresholds and because the minimum detectable signal at maximum range is about 0 dBZ. Note that the true cloud height will extend above the radar-detected height. This may be by a significant amount in the lower to midtroposphere and less near the tropopause, although the results of combined radar and photogrammetry of Kingsmill and Wakimoto (1991) suggest that this will be less than about a kilometer for isolated cells.

An example of a reflectivity field with the identified cell locations is shown in Fig. 1. While every cell with reflectivities greater than 45 dBZ is active convection, the same may not always be true when a lower threshold is used. With the lower threshold, stratiform regions of squall lines may have reflectivity greater than 35 dBZ, particularly if a bright band is present. To test for contamination a convective–stratiform classification procedure using the algorithms of Steiner et al. (1995) was performed on the radar images. Only about 4% of the cell tracks contained at least one time when the classification showed as stratiform. Lower-reflectivity thresholds than 35 dBZ are not used because of problems associated with the radar bright band and decayed cells merging causing significant detection and tracking errors. This limitation will clearly exclude the sampling of nonprecipitating and very lightly precipitating congestus clouds.

The TITAN analysis is not without its problems and limitations. About a half of the detected cells are not found on the next volume scan (i.e., a cell "lifetime" of 10 min or less). While it is certainly possible that a significant fraction (probably most) of these single detection cells only just reach the reflectivity thresholds and these short lifetimes are real, there must be additional cases where the cells have been misidentified. It is worth noting that the fraction of short lifetime cells is similar for both the 35- and 45-dBZ datasets. Also, cell-tracking errors are expected to be relatively small since the cell movement is relatively slow in the Tropics because of the low wind speeds (see, e.g., Keenan and Carbone 1992). The cell concentration is much less in the 45-dBZ data though, so that misidentifications may be expected to be relatively rare, so that many of the short lifetime cells may be genuine. In the analysis to follow, we will discriminate the statistics for these single detection cells and datasets where the cells have been tracked over several volume scans. There is also the potential for single cells to oscillate in intensity about the cell reflectivity threshold and be counted more than once, but such cases are again probably few.

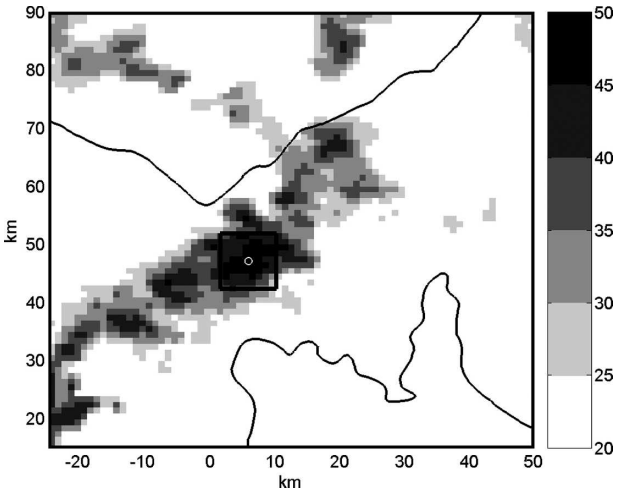

FIG. 1. Radar reflectivity field at a height of 2 km above ground at 0050 UTC 22 Dec 2003. The scales are from a Cartesian grid centered on the radar. The TITAN cell location using a 45-dBZ threshold is shown as a black square. The reflectivity profile in a column above this rectangle is used for the calculations in this paper. The thin solid lines mark Melville Island to the north and the mainland coast to the south.

There are also issues with regard to the spatial resolution of the radar at long range (a 1° beamwidth corresponds to a height smearing of about 2 km at 100-km range) and limitations at close range because of the coarse elevation angle stepping in the vertical at high angles and a "cone of silence" corresponding to the 42° maximum elevation angle. Histograms of storm tops were examined as a function of radar range and there did not appear to be any significant bias. As will be shown, there is some tendency for storms to form near the radar in the monsoon, but this may be associated with enhanced convergence associated with onshore flow.

We use the data collected during November 2003–February 2004. This period is chosen partly for convenience as this was the first season that we used TITAN operationally over northern Australia and partly because it includes extended monsoon periods (17 December 2003–16 January 2004 and 1–17 February 2004) as well as a buildup (up to 16 December 2003) and a break period (17–30 January 2004) allowing us to compare the cell characteristics for these archetypal situations. The cold point tropopause in the soundings during this period was approximately 17 km. The profiles start to show an increase in stability somewhat lower,

with a break in slope of the potential temperature at about 16 km.

While the main focus will be on radar data, this paper will make use of sounding and numerical weather prediction model data. The soundings that will be used are the operational 12-hourly (0000 and 1200 UTC) soundings from the Darwin airport. The numerical weather prediction (NWP) analyses are from the Bureau of Meteorology operational Tropical Limited-Area Prediction System (TLAPS; Puri et al. 1998).

3. Background meteorology

Darwin has a pronounced wet season occurring between approximately October and April. The monsoon season can be defined by low-level westerly winds and convection with oceanic characteristics but includes break periods with low-level easterly winds when the convection is characteristic of coastal and continental convective systems (e.g., Holland 1986; Drosdowsky 1996). These papers showed that simple algorithms provide a robust signature of monsoon versus break signatures and that more complex definitions that included area-averaged cloudiness arrived at very similar onset dates. In this manuscript we simply defined the monsoon periods as having a westerly wind component at 700 hPa in Darwin sounding data where the winds were smoothed by a 3-day running mean. These produced a neat separation in terms of storm distribution and propagation. The resulting statistics are robust for variations of onset days by a day or so. The early part of the buildup is characterized by relatively weak and shallow storms when compared with the "mature" part of the buildup just prior to the monsoon onset. It is during this mature phase when the storms reach their greatest intensity (Hamilton et al. 2004). The storm characteristics during this mature phase and during breaks in the monsoon are similar, so we will be compositing data beginning from 21 November 2004. It was found that the statistics from this time were stable while the earlier period was characterized by relative weak and shallow storms. Each wet season has these monsoon and break periods interspersed. The cells in the break periods have a strong diurnal modulation with a distinct afternoon maximum, frequently with echo tops reaching and overshooting the tropopause and are often very electrically active indicating very strong vertical motions near the freezing level (e.g., Keenan and Carbone 1992). The highest rainfall in the area occurs in January and February when monsoon conditions dominate. Monsoon convection is oceanic in character, with warm rain processes being important. The monsoon cells are less electrically active than during break periods and have radar reflectivities that decrease in height more rapidly than break season continental-type convection; and the diurnal cycle has a relatively weak nocturnal maximum (Keenan and Carbone 1992; Keenan et al. 1989; Hamilton et al. 2004). These systems are more typical of what occurs across the Maritime Continent and the ITCZ. However, as will be shown, the monsoon clouds also reach the tropopause, and the area of active convection is typically larger during the monsoon compared with buildup and "break" periods.

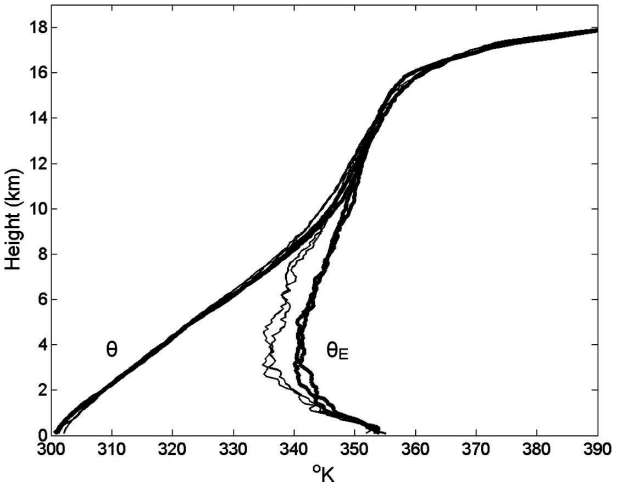

FIG. 2. The median profiles of potential temperature and equivalent potential temperature from Darwin operational soundings. The heavy lines represent the first two monsoon periods and the thin lines are during the buildup and the first break period.

It has been well observed that the thermodynamic characteristics of radiosonde ascents are significantly different in the two regimes (e.g., McBride and Frank 1999) although the distribution of the CAPE, and equivalent potential temperature (θ_E) profiles are strongly overlapping (e.g., Fig. 7 of McBride and Frank 1999). Keenan and Carbone (1992) observed that storms occurred in a wide variety of shear and CAPE conditions. The McBride and Frank paper showed that on average there was slightly more CAPE during the breaks, but there are major differences in the midlevel humidity structure with θ_E being markedly warmer in the midlevels during the monsoon. (Fig. 2). The surface temperatures are slightly warmer (approximately 1°–2°C) during the buildup and break periods compared with the monsoon. When CAPE and the convective inhibition (CIN) were calculated from the Darwin soundings, it is seen that the distributions of these variables are quite broad and the mean values for the different large-scale regimes were not significantly different. This result may be because of the large variations

in CAPE due to small spatial-scale variations in humidity (e.g., Weckwerth 2000).

Figure 3 shows a time series of the 500-hPa humidity and vertical motion over Darwin as analyzed with the Bureau of Meteorology TLAPS system along with the number of cells per day over the 2003–04 wet season. This time series clearly shows that the monsoon periods have both mean upward motion and moister midlevels than the breaks. The temporal variations of the mixing ratio are highly coherent with height although there are higher mean values in the lower levels as may be expected (not shown). There is a hint that increased convective activity is associated with a moistening of the midlevels, but this may also be associated with advection rather than detrainment. However, note that the dynamical nudging approach of Davidson and Puri (1992) is used in the data assimilation of the TLAPS model, and it will impose vertical motions consistent with the observed cloud cover.

The different regimes generally show a strong differentiation with respect to the mean vertical motion. Figure 4 shows the mean vertical motion from the TLAPS analyses at 0000 and 1200 UTC for several grid points around Darwin. There is a clear dichotomy between the buildup and break profiles and the monsoon profiles. The buildup profiles show mean upward motion up to 3 km over the land and descent over the water with indications of a return flow above these levels. This is suggestive of a sea-breeze-type circulation, but neither the model resolution nor the timing of the analyses is ideal for resolving such a circulation. There is a tendency for the vertical motion over the water to have opposing signs to those over the land at higher levels as well. In contrast, the monsoon profiles show upward motion throughout the troposphere that is much stronger than during the buildup and break phases. There is still a tendency for a low-level upward maximum over the land but with a midtropospheric maximum that is stronger over the oceanic grid points. As may be expected, the mixing ratio is anomalously high in regions of substantial upward motion (not shown). One feature of note is an increase in the midlevel (~5 km) mixing ratio during the buildup compared with the overall average indicating perhaps some impact from the increasing amount of convection that will be discussed next. The vertical motion signal is consistent with the environment being more supportive of widespread convection in the monsoon periods. The vertical motion in the second, short break was similar in shape, but weaker than the monsoon cases and the midlevel moistening less (not shown), but this event also had a relatively weak signature in terms of the storm numbers.

The number of (35 dBZ) cells per day and intense (45 dBZ) cells per day across the 300-km-diameter domain are also shown in Fig. 3 (as well as the height distribution for cells within the 256 km $\times$ 256 km grid). The number of intense cells is about 10% of the total number of cells, but the time evolution of the curves is very different. These curves are both smoothly varying in time, and there is a tendency for more storms during the period of large-scale ascent although this is not so evident during the second monsoon period, which was more suppressed. The large number of intense cells on 9 January is associated with a single large squall line indicating the possibility that the overall statistics can be affected by singular large events.

The number of intense cells per day is almost anticorrelated with the large-scale ascent. A possible interpretation of this when we start to examine the radar data is that the monsoon periods, with their large-scale ascent, are favored for allowing widespread convection and therefore more cells, but these are on average weaker and there is a lower number of intense cells. However, during the buildup and break conditions there is more inhibition to free convection because of the midlevel descent so that there is a greater requirement for surface heating to build up potential instability and a need for stronger forcing mechanisms to initiate the convection producing less frequent storms, but more intense cells. This is not clear in the CIN calculated from raw soundings, but high spatial variability of low-level moisture may mask this.

4. Cell characteristics

This section focuses on the maximum size and height that the thunderstorm cells obtain and the cell duration. The two thresholds approximate the areas of precipitating convection (35 dBZ) and the areas of intense convection (45 dBZ) with about 10 times as many cells in the former class. Note that these thresholds automatically exclude the very numerous shallow nonprecipitating clouds that are a ubiquitous feature in satellite imagery as well as much of the cumulus congestus that is visible, but produce little rain. The rainfall accumulations estimated using a Marshall–Palmer Z–R relation show that the 35-dBZ cells include about 40% of the total rainfall while the 45-dBZ cells include only about 10% of the total rain. The total rain was estimated by summing the rainfall across the 256 km $\times$ 256 km field, while the cell rainfall was calculated using the summation of pixels within the cells. The 40% figure for the 35-dBZ cells means that most of the convective precipitation has been captured as about 40%–60% of the precipitation in the Tropics is from stratiform rain that is mostly made up of decayed convective cells (e.g.,

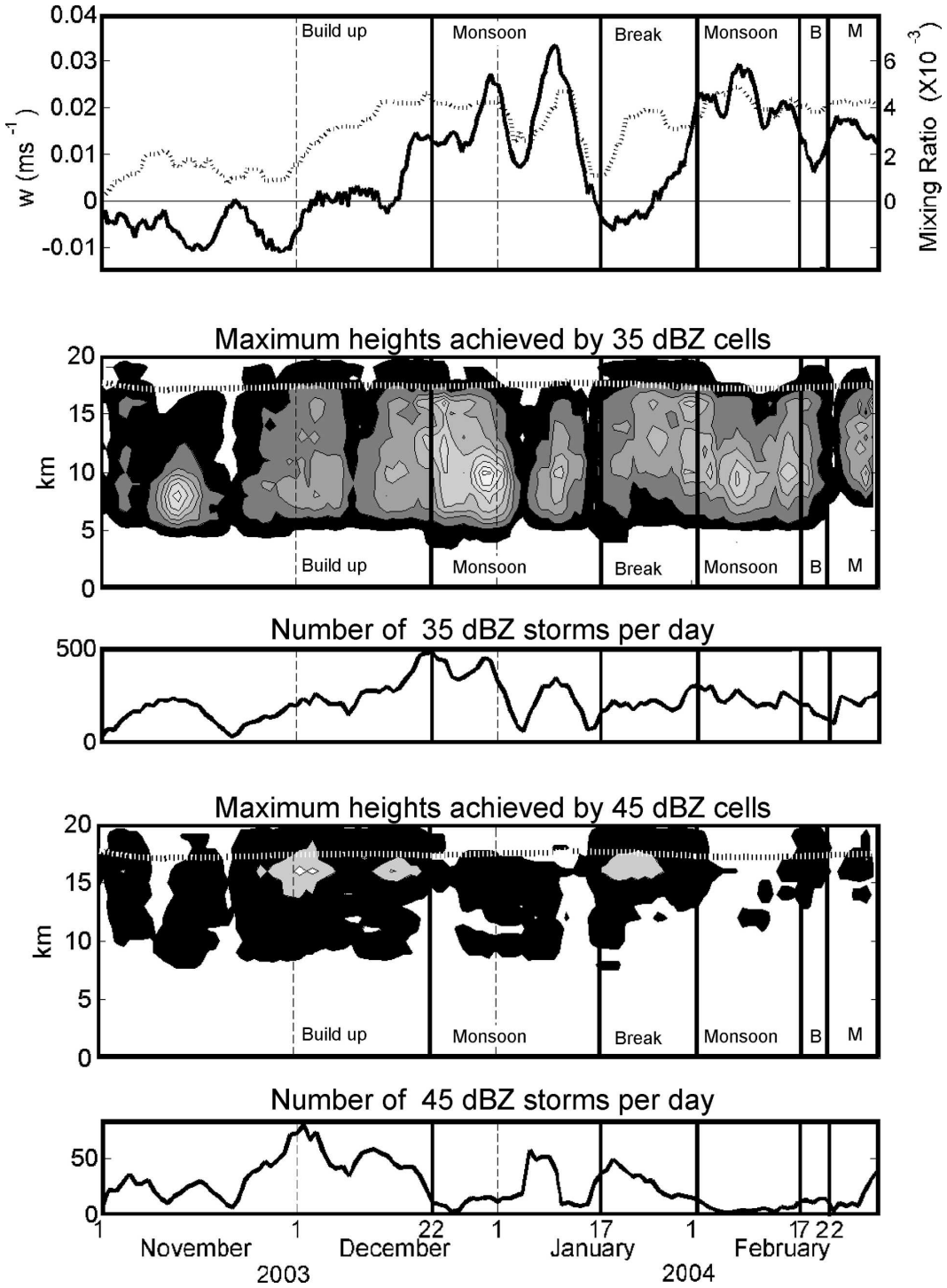

FIG. 3. (top) Time series of the operational mesoscale analysis of midtropospheric vertical velocity (solid line) and mixing ratio (dotted line) along with a summary of the storm activity. This takes the form of the total number of cells within the 300-km-diameter domain and a panel showing contours of the frequency of cell maximum heights reaching a particular value in increments of 1 km day^{-1} in the smaller 256 km $\times$ 256 km domain. The data have been passed through a 5-day running mean to smooth the results. Contours are drawn every 5 cells per day and the shaded region marks the height–time range with detected cells. The dashed line near 17 km is the height of the tropopause defined as the minimum tropospheric temperature. This is based on soundings from Darwin smoothed over 10 days. Data from the two-cell threshold definitions are displayed, with (two middle panels) 35 dBZ representing most cells and (bottom two) the 45 dBZ representing the subset of intense cells. The heavy vertical lines mark the monsoon onset (22 Dec 2003), first break (17 Jan 2004), the onset of the second monsoon burst (1 Feb 2004), and a second break (17 Feb 2004). Monsoon conditions returned on 22 Feb 2004.

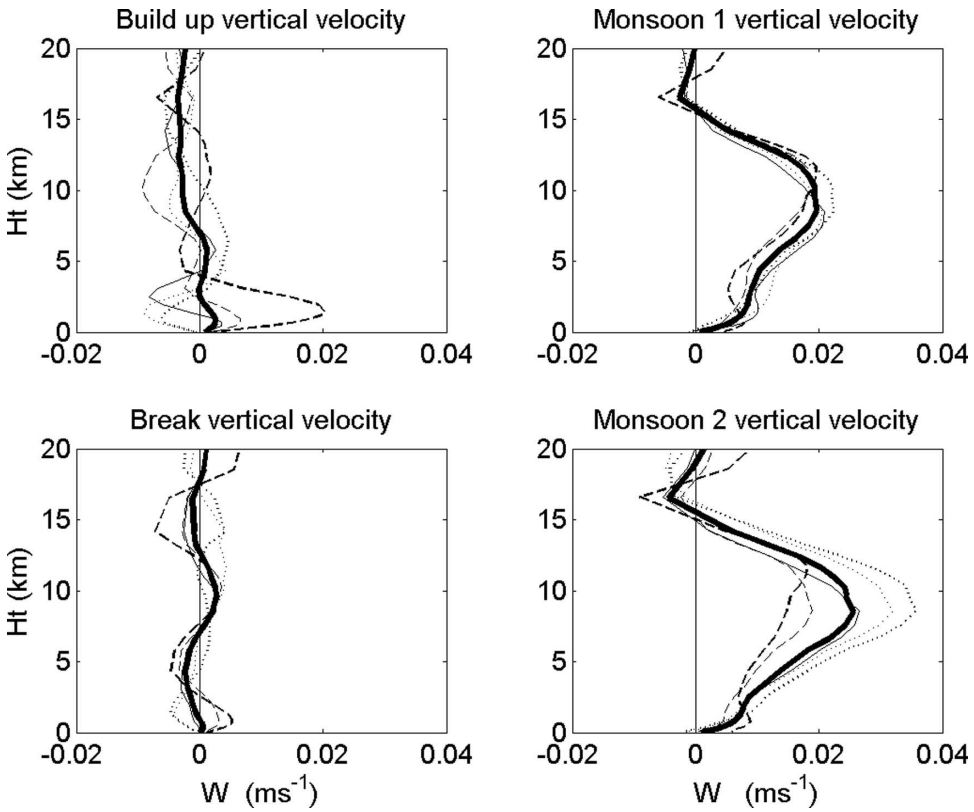

FIG. 4. Profiles of mean vertical motion for five grid points around Darwin from the Bureau of Meteorology "tropical" LAPS model during the buildup, break, and two monsoon phases. The dashed lines are for land profiles, the dotted lines are over the water, and the thin solid line is for a coastal pixel. The heavy black line is the mean. Analyses at 0000 and 1200 UTC are included in the average.

Houze and Cheng 1977; Steiner and Houze 1998). However, the intense cells represent the bulk of the cases where the storm cells reach the upper troposphere or overshoot the tropopause and are thus very important in their potential effects on the tropical transition layer (Folkins 2002). The analysis partitions cells into monsoon and break conditions as is described above. The area-averaged rainfall accumulation in the monsoon period was about twice that of the break, but there were more intense cells per day during the break.

A time–height cross section of the cell tops for both reflectivity thresholds is shown in Fig. 3. These are smoothed by a 5-day running mean. The first burst of deep activity is after 20 November. The earlier peak in the 35-dBZ cell numbers in Fig. 3 were characteristic of the early stage of the buildup with relatively few deep intense cells, whereas the mature buildup period is characterized by a substantially higher fraction of intense and deep storms. It is also interesting to note that it is only after the numbers of intense storms grew that the midlevel humidity begins to increase. The relatively dry midlayers may limit cloud growth by the entrainment of very dry air, although there is a distinct "chicken and egg" issue here. From November through to the monsoon onset, the number of storms reaching large intensities and height increase. The characteristics in the buildup from 20 November and the break periods show quite similar features, in both the height distribution of the cells and intensity. The next feature to note is the distinct drop in both the number of intense cells and the maximum height reached by the convective cells in the monsoon periods. Also, the first, long monsoon burst has two distinct active phases separated by a suppressed period that coincided with a distinct weakening of the low-level westerly wind. The first of the active periods was associated with a tropical cyclone in the Gulf of Carpentaria to the east and Darwin was being influenced by its outer circulation. The second monsoon period had no cells reaching the 45-dBZ threshold with the smoothing of the data accounting for the overlap of the contours into that period.

These results are consolidated by constructing histograms of the storm heights for the monsoon periods as well as the buildup period after 21 November and the

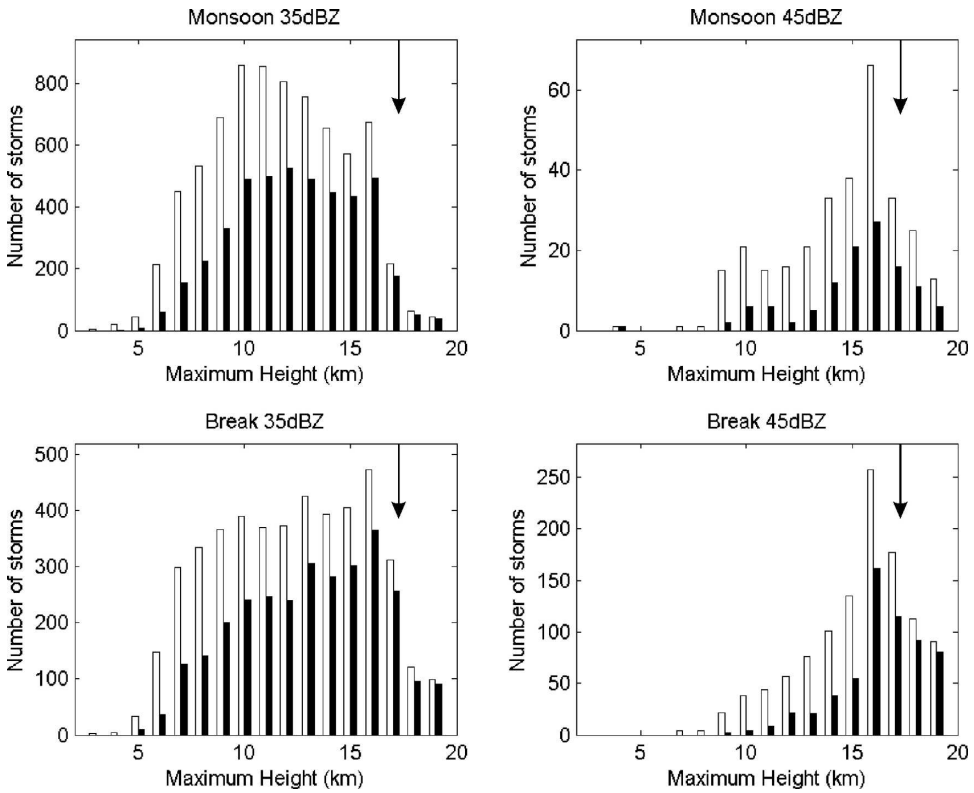

FIG. 5. Histograms of the maximum height that convective cells defined by possessing a volume of reflectivity greater than the (left) 35- or (right) 45-dBZ reach for the monsoon and break periods along with the buildup after 20 November. A 5-dBZ threshold was used here to define the cell top. The open columns are for all cell detections while the filled columns are for cells that persist (with reflectivity greater than the 35- or 45-dBZ threshold) for longer than 10 min.

break periods. Figure 5 shows histograms of the maximum height that individual cells reach at any stage of their evolution for these two periods using a 5-dBZ threshold to define a cloud top for the 35- and 45-dBZ cells. There are clearly differences in the populations of the cell tops in that essentially all the intense cells during the break reach near the tropopause with a significant population of overshooting tops. The monsoon cloud tops often also extend to the tropopause transition layer (TTL) but steadily decrease in numbers as the tops approach the cold point tropopause, but again there are some overshooting tops. There is a substantial population of 35-dBZ cells with tops between 8 and 15 km. This is superficially consistent with the notion of May and Rajopadhyaya (1999) and Johnson et al. (1999) that there exists a population of cells in the Tropics that have a maximum height in the midtroposphere for the subset of intense cells, but examination of the distributions that include weaker cells reveals little evidence of different modes within the distribution. If a lower-reflectivity threshold such as 35 dBZ is used to define a cell, the peak in the height distribution is near 10 km in the monsoon period and in the upper troposphere in the break.

A superposition of the monsoon and break clouds would give some hint of the upper two peaks of the convective distribution, but this is clearly associated with two distinct regimes and is different from the observations discussed by Johnson et al. (1999), which was for oceanic convection only and thus is expected to be similar to the monsoon data alone. Although it must be remembered that these are the radar echo tops and the actual cloud top may be somewhat higher than these altitudes, generally the echo top is within 500 m to 1 km of the cell top (Kingsmill and Wakimoto 1991). Even given this uncertainty, it is highly likely that there are more cases of penetrating convection in the break periods, but on a global or regional basis, it must also be kept in mind that there is a much greater area of oceanic-type convection than for the coastal/continental type. Detailed satellite studies are needed to pursue this issue further. One inference of this analysis is that it is likely that the updraft speed within the intense cores is less in the monsoon compared with the break as

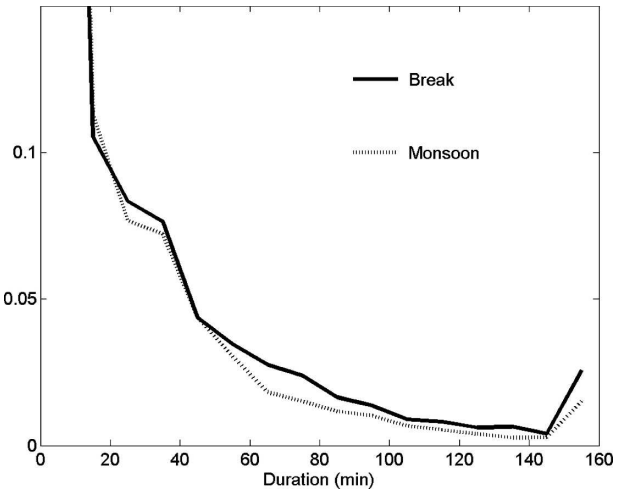

FIG. 6. The probability distribution of cell lifetime for monsoon (dotted) and break (solid) 35-dBZ cells. The peak at 150 is partly due to the binning of all times greater than 140 min and the limits associated with very long lived cells propagating outside the domain.

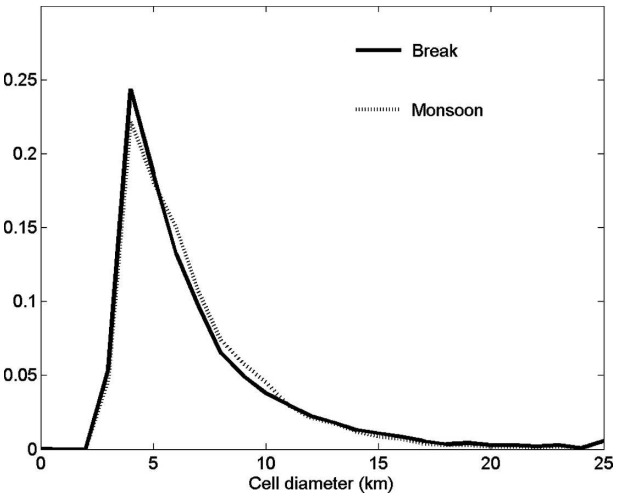

FIG. 7. The 35-dBZ probability distribution of the maximum storm area during the cell lifetime for break (solid) and monsoon (dotted) cells. The cell area is determined from the raw TITAN tracks, not the rectangle around the cell.

there is less penetration of the tropopause and more cells detraining at lower altitudes. This is consistent with the weaker vertical motions around the freezing level inferred by lightning studies and the vertical profiles of reflectivity (e.g., Keenan and Carbone 1992).

Overall there is little support for the concept of distinct populations of cells confined to about the freezing level and a second distinct peak near the tropopause in these data. Rather the impression is a continuous distribution of cloud tops that have a peak that shifts toward larger heights as the cells with lower reflectivity are excluded, although in the monsoon there is some indication of a small peak in intense cells around 10 km in height as well as near the tropopause. If weakly precipitating congestus was added to the dataset, it would likely move the peak to near the freezing level and the 35-dBZ cells would constitute the higher reflectivity tail of the distribution and the 45-dBZ cells, the extreme part of the distribution.

Other products that come from the TITAN analyses are the cell lifetimes and sizes. As noted in the previous section, there are many cases with very short lifetimes above the respective reflectivity thresholds (e.g., Fig. 6). The probability distribution of cell lifetimes is approximately exponential with a mean time of about 30 min for cells that are tracked for more than one time step. The single detections appear about twice as often as one would expect for an exponential fit to the remaining data. Within the 35-dBZ cells there is also a clear correlation between the cell lifetime and storm maximum height. It must also be kept in mind that the cloud lifetime may be considerably longer than our "cell lifetimes" as a given cloud may only satisfy our cell criteria for a short part of its evolution.

The distribution of cell diameters has a mode at about 5 km for both the 35- and 45-dBZ thresholds reflecting a preponderance of small cells and is almost independent of the storm regime (Fig. 7). Of course, the 35-dBZ cell threshold distribution extends to larger diameters. Here it must be remembered that the TITAN cell definition effectively precludes cells smaller than about 3 km in diameter and thus truncates the distribution. The break season cells tend to be slightly smaller, but last a little longer than the cells in the monsoon. The distributions are similar, but significantly different on statistical tests. Sauvageot et al. (1999) used exponential fits to the size distributions and our data are consistent with their results, but with a smaller slope so that we have more larger cells and of course our distributions are truncated at small diameters.

The observed size distributions cover similar size ranges to the lognormal distributions observed at a number of locations by Lopez (1977), as well as in GATE (LeMone and Zipser 1980) and Potts et al. (2000) for midlatitude cells, but the distribution shape is more skewed than lognormal.

5. Discussion and conclusions

A focus of the analysis described above was to examine the operational radar data for evidence of multimodal distributions of echo height. Data were analyzed during the two regime types typically seen in Darwin. These are the buildup or break regime and the

monsoonal regime. The characteristics of the convection observed in these regimes are continental and oceanic, respectively. It has long been pointed out that the continental-type convection is more intense in terms of the electrical activity, reflectivity structure, etc. The distribution of storm heights has been systematically quantified with objective cell definitions and detections here, and we see a shift toward taller cells at all intensities and a higher probability of tall, intense storms during the buildup compared with monsoonal conditions. There are also only small differences in typical storm size and lifetime, with the buildup cells typically smaller, but longer lived. This is interesting because it has been argued that updraft size may scale as boundary layer depth (which is greater in the break compared with the monsoon with its oceanic trajectory), although GATE updrafts were of similar size to those observed during the Thunderstorm project in the midwestern section of the United States (Zipser and LeMone 1980). This would argue for larger cells during the break. The break season cells do persist for slightly longer than the less intense monsoon cells, and this may be a reflection of the requirement for stronger forcing to initiate convection and the weaker cells decaying to stratiform rain more quickly. Certainly we see higher average total rainfall and a much larger fraction of stratiform rain in the monsoon.

Within individual regimes, we see no strong support for trimodal distributions of cell maximum heights as hypothesized by Johnson et al. (1999). Rather, these results point toward single-peaked continuous distributions and the mode in the distribution of maximum heights shifts toward larger heights as the cells are conditioned on higher reflectivity. In the context of the Johnson et al. discussion it is not the "congestus peak" that is missing but rather the deep convective peak. The results shown in this paper indicate that the deep convection is the tail of the distribution rather than a separate recognizable peak. This study did not include non- or weakly precipitating congestus clouds, but it would be expected that these would add to the distributions seen in Fig. 5 as moving the peak to higher numbers and lower heights rather than a clearly separate peak. The peak for the moderate intensity rain (35-dBZ cells) for the oceanic convection is quite broad, but is already moved to the peak below 10 km and the shape is broadly consistent with the Houze and Cheng (1977) results that underpin the Johnson et al. analysis. The addition of non- or weakly precipitating cells will almost certainly increase the number of clouds by a large factor and move the peak down toward the freezing level, but this does not imply separate populations of clouds. That said, there is clearly a regime dependence on the height distributions. The height distribution in the early part of the buildup was distinctly different from the mature onset and break periods that in turn were different from the monsoon situation.

A clear result from this analysis is that the subset of intense cells reach significantly higher altitudes and that most reach the tropopause, although there are more lower-altitude cells in the monsoon. Future work will include an examination of which cells contribute most to the cirrus anvils that accompany periods of storm activity—the many shallow cells or the few longer-lived deep cells. Another area of examination is how the cell characteristics vary with time of day and the role and frequency of congestus as the overall storm structures evolve. A more detailed study of the differences in cells that undergo mergers will also be undertaken. It has been hypothesized that cells that merge undergo a geometric increase in storm size and rainfall production in this region (Simpson et al. 1993). A preliminary analysis shows that merged cells on average are somewhat larger and almost by definition tend to persist longer than the isolated cells. They also tend to have higher maximum reflectivities by a few dBZ. This work will be extended to explore cell evolution with and without merger processes.

Acknowledgments. The assistance and support of Rod Potts and Alan Seed in collecting these data has been vital. Discussions with Andreas Vallgren on the impacts of mergers on cell intensity and structure are greatly appreciated. This work has been partially supported by the U.S. DOE Atmospheric Radiation Measurement (ARM) program.

REFERENCES

Davidson, N. E., and K. Puri, 1992: Tropical prediction using dynamical nudging, satellite-defined convective heat sources, and a cyclone bogus. *Mon. Wea. Rev.,* **120,** 2501–2522.

Dixon, M., and G. Wiener, 1993: TITAN: Thunderstorm Identification, Tracking, Analysis, and Nowcasting—A radar-based methodology. *J. Atmos. Oceanic Technol.,* **10,** 785–797.

Drosdowsky, W., 1996: Variability of the Australian summer monsoon at Darwin: 1957–1992. *J. Climate,* **9,** 85–96.

Folkins, I., 2002: Origin of lapse rate changes in the upper tropical troposphere. *J. Atmos. Sci.,* **59,** 992–1005.

Goeke, S., M. C. Robles, R. M. Rauber, and J. B. Jensen, 2005: Radar analysis of long-lived trade wind cumulus clouds from the Rain in Cumulus over the Ocean experiment (RICO). Preprints, *32d Conf. on Radar Meteorology,* Albuquerque, NM, Amer. Meteor. Soc., CD-ROM, J3J.6.

Hamilton, K., R. A. Vincent, and P. T. May, 2004: The DAWEX field campaign to study gravity wave generation and propagation. *J. Geophys. Res.,* **109,** D20S01, doi:10.1029/2003/JD004393.

Holland, G. J., 1986: Interannual variability of the Australian summer monsoon at Darwin: 1952–82. *Mon. Wea. Rev.,* **114,** 594–604.

Houze, R. A., Jr., and C.-P. Cheng, 1977: Radar characteristics of tropical convection observed during GATE: Mean properties and trends over the summer season. *Mon. Wea. Rev.,* **105,** 964–980.

Johnson, R. H., T. M. Rickenbach, S. A. Rutledge, P. E. Ciesielski, and W. H. Schubert, 1999: Trimodal characteristics of tropical convection. *J. Climate,* **12,** 2397–2418.

Keenan, T. D., and R. E. Carbone, 1992: A preliminary morphology of precipitation systems in tropical northern Australia. *Quart. J. Roy. Meteor. Soc.,* **118,** 283–326.

——, J. McBride, G. Holland, N. Davidson, and B. Gunn, 1989: Diurnal variations during the Australian Monsoon Experiment (AMEX) Phase II. *Mon. Wea. Rev.,* **117,** 2535–2553.

Kingsmill, D. E., and R. M. Wakimoto, 1991: Kinematic, dynamic, and thermodynamic analysis of a weakly sheared severe thunderstorm over northern Alabama. *Mon. Wea. Rev.,* **119,** 262–297.

LeMone, M. A., and E. J. Zipser, 1980: Cumulonimbus vertical velocity events in GATE. Part I: Diameter, intensity, and mass flux. *J. Atmos. Sci.,* **37,** 2444–2457.

Lopez, R. E., 1977: Some properties of convective plume and small fair weather cumulus fields as measured by acoustic and lidar sounders. *J. Appl. Meteor.,* **16,** 861–865.

May, P. T., and D. K. Rajopadhyaya, 1999: Vertical velocity characteristics of deep convection over Darwin, Australia. *Mon. Wea. Rev.,* **127,** 1056–1071.

——, and T. D. Keenan, 2005: Evaluation of microphysical retrievals from polarimetric radar with wind profiler data. *J. Appl. Meteor.,* **44,** 827–838.

McBride, J. L., and W. M. Frank, 1999: Relationships between stability and monsoon convection. *J. Atmos. Sci.,* **56,** 24–36.

Petersen, W. A., and S. A. Rutledge, 2001: Regional variability of tropical convection: Observations from TRMM. *J. Climate,* **14,** 3566–3586.

Potts, R. J., T. D. Keenan, and P. T. May, 2000: Radar characteristics of storms in the Sydney area. *Mon. Wea. Rev.,* **128,** 3308–3319.

Puri, K., G. S. Dietachmayer, G. A. Mills, N. E. Davidson, R. Bowen, and L. W. Logan, 1998: The new BMRC Limited Area Prediction System, LAPS. *Aust. Meteor. Mag.,* **47,** 203–223.

Rutledge, S. A., E. R. Williams, and T. D. Keenan, 1992: The Down Upper Doppler and Electricity Experiment (DUNDEE): Overview and preliminary results. *Bull. Amer. Meteor. Soc.,* **73,** 3–16.

Sauvageot, H., F. Mesnard, and R. S. Tenorio, 1999: The relation between the area-average rain rate and the rain cell size distribution parameters. *J. Atmos. Sci.,* **56,** 57–70.

Seed, A. W., and G. G. S. Pegram, 2001: Using Kriging to infill gaps in radar data due to ground clutter in real-time. *Proc. Fifth Int. Symp. on Hydrological Applications of Weather Radar,* Kyoto, Japan, Disaster Prevention Research Institute, Kyoto University, 73–78.

Short, D. A., and K. Nakamura, 2000: TRMM radar observations of shallow precipitation over the tropical oceans. *J. Climate,* **13,** 4107–4124.

Simpson, J. S., T. D. Keenan, B. Ferrier, R. H. Simpson, and G. J. Holland, 1993: Cumulus merging in the maritime continent region. *Meteor. Atmos. Phys.,* **51,** 73–99.

Steiner, M., and R. A. Houze Jr., 1998: Sensitivity of monthly three-dimensional radar-echo characteristics to sampling interval. *J. Meteor. Soc. Japan,* **76,** 73–95.

——, ——, and S. E. Yuter, 1995: Climatological characterization of three-dimensional storm structure from operational radar and rain gauge data. *J. Appl. Meteor.,* **34,** 1978–2007.

Toracinta, E. R., D. J. Cecil, E. J. Zipser, and S. W. Nesbitt, 2002: Radar, passive microwave, and lightning characteristics of precipitating systems in the Tropics. *Mon. Wea. Rev.,* **130,** 802–824.

Weckwerth, T. M., 2000: The effect of small-scale moisture variability on thunderstorm initiation. *Mon. Wea. Rev.,* **128,** 4017–4030.

Williams, E. R., S. A. Rutledge, S. G. Geotis, N. Renno, E. Rasmussen, and T. Rickenbach, 1992: A radar and electrical study of tropical "hot towers." *J. Atmos. Sci.,* **49,** 1386–1395.

Zipser, E. J., and M. A. LeMone, 1980: Cumulonimbus vertical velocity events in GATE. Part II: Synthesis and model core structure. *J. Atmos. Sci.,* **37,** 2458–2469.